

Honeycomb supported perovskite catalysts for ammonia oxidation processes

L.A. Isupova*, E.F. Sutormina, N.A. Kulikovskaya, L.M. Plyasova,
N.A. Rudina, I.A. Ovsiyannikova, I.A. Zolotarskii, V.A. Sadykov

Boreskov Institute of Catalysis SB RAS, pr. Lavrentieva, 5, Novosibirsk 630090, Russia

Available online 12 July 2005

Abstract

Pechini route (M.P. Pechini. U.S. Patent no. 3,330,697 (1967)) was used for supporting perovskite – like systems LaBO_3 ($B = \text{Mn, Fe, Co, Ni, Cu}$) on thin-wall (0.35 mm) cordierite honeycomb support with low thermal expansion coefficient to prepare stable to thermal shocks supported catalysts for high-temperature processes of ammonia oxidation into NO in nitric acid production. In this preparation route, perovskites (2–6%) have nearly uniform distribution in the walls as well as form surface grainy perovskite layer 2–3 μm thick that may be also important for the high temperature processes occurring at short contact times. Cordierite supported lanthanum manganite and cobaltite are the most active in the reaction of ammonia oxidation into NO especially when supported twice or on a secondary sublayer (Ln_2O_3 , ZrO_2 , MeO , LaBO_3).

© 2005 Elsevier B.V. All rights reserved.

Keywords: Ammonia oxidation; Perovskites; Honeycomb cordierite-supported catalysts

1. Introduction

High-temperature catalytic processes such as deep and partial oxidation of methane, its autothermal reforming, fuels combustion, ammonia oxidation into NO etc are now among the most rapidly developing fields in heterogeneous industrial catalysis. Complex oxides with perovskite structure were shown to be promising for such applications [1–9]. For those processes occurring at short contact times, the monolith honeycomb shape of catalysts is often required [10]. There are two types of monolith catalysts – bulk (consisting mainly of the active component) and supported (impregnated on an inert substrate) ones. Earlier two types of bulk honeycomb monolith oxide catalysts for ammonia oxidation process were developed by the Boreskov Institute of catalysis, which are now commercially used in nitric acid plants [11–15]. An aspect of material thermal expansion coefficient (TEC) plays an important role for monolith honeycomb catalysts. Bulk perovskite-based catalysts show

rather high TEC. Another traditional approach in technology of monolithic catalysts preparation consists in supporting the active components on the refractory monolithic carrier [16–20]. The cordierite (frame structured material with chemical composition $2\text{MgO} \cdot 2\text{Al}_2\text{O}_3 \cdot 5\text{SiO}_2$) carrier is characterized by a low thermal expansion coefficient ($2 \times 10^{-6} \text{ 1/K}$ [21]) that is very important for catalyst stability to thermal cycles. This paper deals with preparation and characterization of perovskites supported on a cordierite honeycomb carrier as catalysts for ammonia oxidation. The impregnation method based on Pechini route was used for catalysts preparation [22,23].

2. Experimental

2.1. Catalyst preparation

The honeycomb cordierite support was made by extrusion of plastic paste (prepared from a talc, a clay, alumina ($\text{Al}_2\text{O}_3 \cdot n\text{H}_2\text{O}$) taken in a required ratio and ethylene

* Corresponding author. Tel.: +7 383 2 30 87 63; fax: +7 383 2 30 80 56.
E-mail address: isupova@catalysis.nsk.su (L.A. Isupova).

glycol water solution) followed by drying and calcinations at 1160 °C for 4 h. The resulted monoliths had triangular channels (2.2 mm side) with wall thickness of 0.35 mm, specific surface area 0.7 m²/g and total pore volume 0.2 cm³/g. The void fraction of the support is 0.53. Supported perovskites LaMeO₃ (Me = Mn, Co, Fe, Ni, Cu) were prepared by impregnation of the monoliths by solutions of nitrates salts with added ethylene glycol and citric acid. The procedure looks as follows. Solutions (20 ml) of nitrate salts (room temperature saturated nitrate solutions were mixed in required proportions) with added citric acid (8 g in 4 ml) and ethylene glycol (2.5 ml) were prepared and heated up to 50 °C. Monolith substrates cut as cylinders with diameter 21–22 mm and 50 mm in height were dipped into solution for 5–10 min. Then samples were taken out of the solution, blown out by air, dried in the air and calcined at 900 °C for 4 h. During drying stage, at 100–200 °C, a film of polymerized metal–ether complexes strongly adhering to the monolithic support walls is formed on internal and external surfaces. After annealing at temperatures exceeding 500 °C, the organic residue is burned, and grainy porous perovskite supported layer emerges. For comparison, supported simple MeO_x (Me = Mn, Co, Fe, Ni, Cu) oxides were also prepared by the same procedure.

To prevent interaction between the active component and support as well as to increase the active component content, a secondary support comprising pure oxides Ln₂O₃ or ZrO₂ was coated by the same impregnation procedure prior to perovskites supporting. The amount of the supported oxide was varied in the range 1–7%.

2.2. Catalyst testing

Ammonia oxidation process was carried out in a quartz tubular reactor with inner diameter 26 mm at temperature 700–900 °C and atmospheric pressure. Samples of honeycomb catalysts in the form of fragments with diameter of 21–22 mm and length of 50 mm were tested. In order to prevent heat losses and operating in an adiabatic regime, the reactor was wound with heating wire and the reactor wall temperature was maintained with Dwyer 2600 temperature controller. The gas temperature above and below the catalyst was measured with chromel–alumel thermocouples. A similar thermocouple was installed in contact with the catalyst wall (in the middle of the monolith) to measure the catalyst temperature. Before the reaction starts up, catalysts were preheated at 700 °C in air for 30 min. Then reaction gases (5% ammonia in the air preheated at 450 °C in a quartz mixer) were flowed through the catalyst with 7.6 l/min flow rate (0.33 m/s at STP). The ignition of the catalyst was determined by the temperature increase.

Outlet gas sampling was performed by a quartz sampler with inner diameter of 3 mm installed within 3–4 mm distance from the catalyst. The gas flow rate through the sampler is about 50 ml/min. The quartz sampling system was heated up to 400 °C to avoid the formation of ammonia

salts and NO₂. An on-line UV spectroscopic method has been used for quantitative analysis of reaction gases [24]. Data were obtained with spectrometer Shimadzu 3101 PC in range of wavelength 200–230 nm with step of 0.05 nm. A continuous flow quartz cell with length of 88 mm was heated to 250 ± 5 °C in order to prevent formation of NO₂. Ammonia (λ_{\max} = 204.8, 208.7, 212.7, 216.9, 221.2 and 224.5 nm), NO (λ_{\max} = 226.0, 213.5 and 203.6 nm) and NO₂ (200 nm) peaks were collected. H₂O, N₂ and N₂O do not absorb in this wave interval.

2.3. Catalyst characterization

The structural and textural properties of supported perovskites were studied by XRD, SEM, X-ray microanalysis, thermal analysis and adsorption measurements.

The X-ray diffraction patterns were obtained with a URD-6 diffractometer using Cu K α - radiation. The 2 θ scan region was 10°–70°. Typical particle sizes were estimated from the broadening of 400 diffraction peak (cubic index) not split due to the hexagonal distortion of the perovskite structure.

The X-ray microanalysis (X-ray beam diameter 1 mm) was carried out on a MAP-3 machine for supported perovskites. The characteristic Me K α (Me = Mn, Fe, Co, Cu, Al) and La L α radiations were registered while moving beam across the wall thickness with step of 10–20 μ m.

The textural properties of supported perovskites were studied by SEM with the BS-350 machine (resolution limit is 5–10 nm).

The thermal analysis (TA) in the air was carried out on the DQ-1500 device. Samples (200 mg) were heated with a ramp of 10 °min^{−1} up to 900 °C under air atmosphere.

The samples pore structure was characterized by the high pressure mercury porometry (HPM) using the Auto-Pore 9200 machine, and the specific surface area (S_{sp} , m²/g) was determined by a routine BET procedure using the Ar thermal desorption data.

Chemical element analysis was determined with atomic absorption spectroscopy (a BAIRD spectrometer).

3. Results and discussions

3.1. The phase composition and texture of supported perovskites

According to X-ray data, the perovskite precursors formed after burning the organic polymer are amorphous, which agrees with the data of [23]. According to TA data heating of these precursors in the air accompanied with thermal effects and weight losses up to 800 °C. Calcination of unsupported LaMeO₃ (Me = Fe, Mn) precursors at 900 °C leads to formation of well-crystallized perovskites particles with typical sizes 80–100 nm. Perovskite structure as well as cobalt, nickel and copper simple oxides admixtures (Co₃O₄

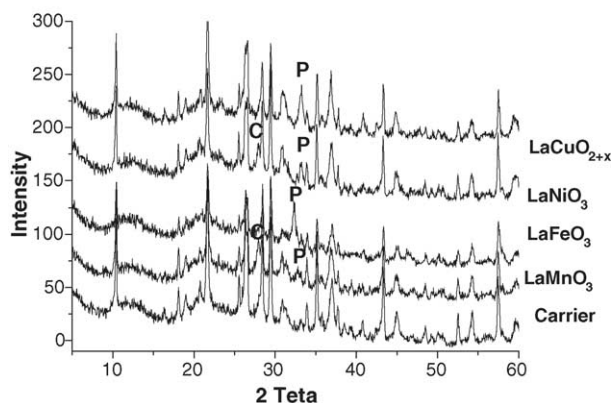


Fig. 1. X-ray diffraction patterns of cordierite carrier and supported perovskite catalysts. P, perovskite peaks; C, lanthanum oxy-carbonate peaks.

[JCPDS 43-1003], NiO [JCPDS 44-1159], CuO [05-0661]), respectively, were revealed in the calcined precursors [23].

In the case of cordierite-supported samples, the mixture of cordierite and perovskite phases was observed after catalyst annealing at 900 °C (Fig. 1). For supported lanthanum manganites and ferrites, the type of structure (hexagonal and orthorhombic, respectively) corresponds to stable modifications included in JCPDS files. In the case of cuprates, nickelates and cobaltites, instead of a stable hexagonal phase, a cubic modification was revealed. Hence, for the latter systems, pronounced interaction between the

active component and support certainly takes places. Most probably, a part of support is dissolved in the acidic polymerized solution at the impregnation stage (e.g. Al cations were detected in the acidic solution after impregnation stage), which can be facilitated by a strong complexation ability of mixed citric acid–ethylene glycol ethers by analogy with [23]. After precursor decomposition and calcination, a part of aluminum cations enters into metastable perovskite-like solid solution, thus affecting their structural properties. In any case, interaction of perovskites phases with cordierite support observed here is not so strong as observed in the case of perovskites supported on corundum [23] or LaMnO₃ supported on γ -Al₂O₃ [16], when after annealing at 1100 °C LaAlO₃ and MnO_x phases were revealed. According to X-ray analysis particle size of supported perovskites is in the range 30–40 nm.

X-ray microanalysis (Fig. 2) revealed that in the case of cordierite supported catalysts prepared using Pechini method, the cations of an active component have a nearly uniform distribution across the wall thickness as well as form a separate layer with thickness 2–3 μ m covering the walls of monolithic support. Taking into account synchronous or asynchronous cations distribution, we can make a conclusion about chemical composition of perovskite phases. The data on the phase composition and element analysis are presented in the Table 1. To summarize, all supported perovskites are really modified with Al to greater or less extent that may strongly influence their activity and selectivity.

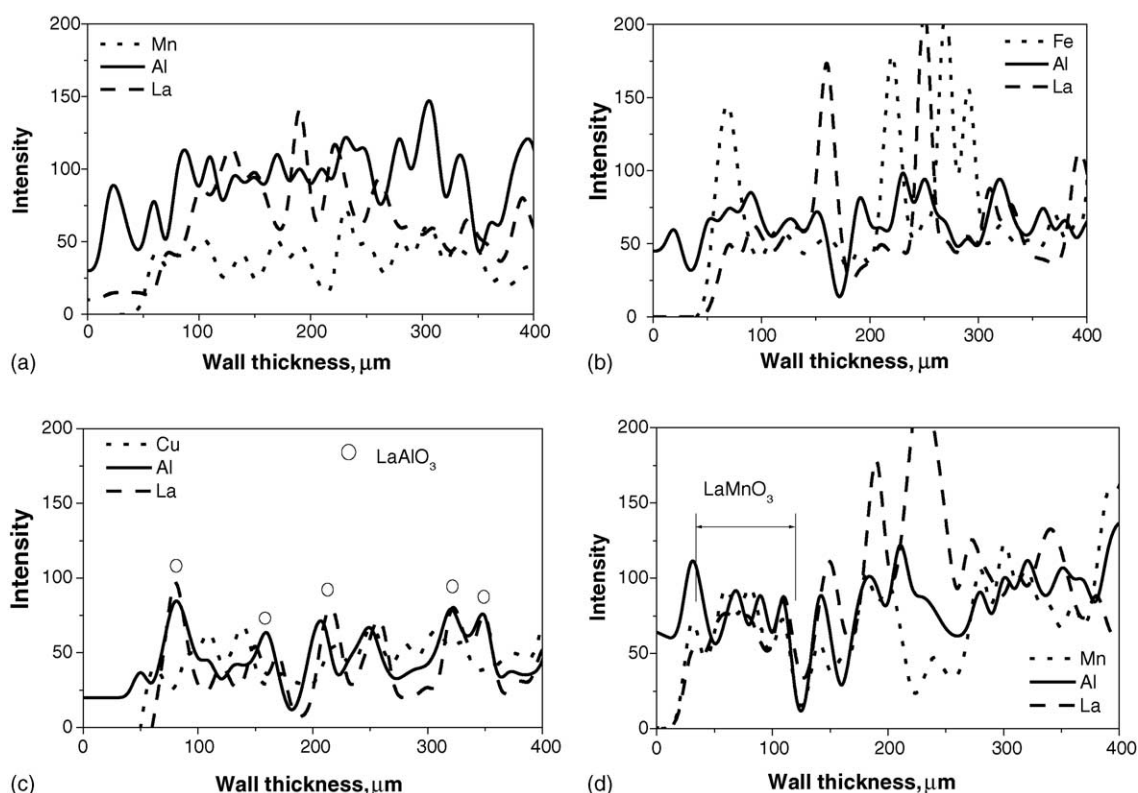


Fig. 2. X-ray element analysis of supported catalysts (a) carrier + LaMnO₃, (b) carrier + LaFeO₃, (c) carrier + LaCuO_{2+x}, (d) carrier + Ln₂O₃ + LaMnO₃.

Table 1

Phase composition of the supported catalysts versus perovskite composition and presence of secondary carrier layer (sublayer) according to X-ray data

No.	Samples nominal composition	X-ray phase analysis of supported oxides	X-ray element analysis on Me distribution across the wall. (Me = Mn, Co, Fe, Ni, Al, La)
1.	Carrier	Cordierite	Quasi uniform Al distribution
2.	Carrier + 7% Ln_2O_3	–	Quasi uniform Al distribution; quasi uniform asynchronous to Al distribution of La across the carrier wall and formation of 2–3- μm surface layer
3.	Carrier + 3.37% LaMnO_3	Perovskite, possible $\text{LaMnO}_3 + (\text{LaO})_2\text{CO}_3$	Quasi uniform distribution of La, Al, and Mn elements; formation of $\text{La}(\text{Mn,Al})\text{O}_3$ perovskite and simple La_2O_3 and MnO_x oxides are not excluded due to partly asynchronous distribution of La and Mn elements
4.	Carrier + 3.38% LaCoO_3	Perovskite, possible LaCoO_3	Quasi uniform La, Al and Co elements' distribution across the carrier wall; formation of $\text{La}(\text{Co,Al})\text{O}_3$ is not excluded
5.	Carrier + 3.33% LaCuO_{2+x}	Perovskite, possible LaCuO_{2+x}	Formation of CuO and LaAlO_3 are not excluded
6.	Carrier + 5.45% LaFeO_3	Perovskite, possible LaFeO_3	Surface of the wall is enriched with $\text{La}(\text{Fe,Al})\text{O}_3$, in the wall formation of La_2O_3 and Fe_2O_3 simple oxides is not excluded
7.	Carrier + 4.95% LaNiO_3	Perovskite, possible $\text{LaNiO}_3 + (\text{LaO})_2\text{CO}_3$	Formation of La_2O_3 , NiO and $\text{La}(\text{Ni, Al})\text{O}_3$ is not excluded
8.	Carrier + $\text{Ln}_2\text{O}_3 + 3\%$ LaMnO_3	–	Surface of the wall enriched with MnO_2 , $\text{La}(\text{Mn,Al})\text{O}_3$ as well as La_2O_3 and MnO_2 , in the wall were detected

According to SEM data (Fig. 3), the supported active component or sublayer form a grainy layer which repeats the carrier surface relief. Separate grains compose this grainy layer, and its morphology is nearly independent upon the calcination temperature. On the wall's cross-section a well-developed internal pore structure of cordierite and the surface layer of supported oxides 2–3 μm in thickness (in agreement with thickness estimation by X-ray microanalysis) is observed (Fig. 4).

For all supported oxides calcined at 900 °C the specific surface area was about 1 m^2/g . The pore size distribution was similar for both supported and unsupported systems with 0.2 cm^3/g integral pore volume.

3.2. Catalytic activity

Estimation of mass transfer rate at testing conditions has shown that when the reaction is limited by ammonia diffusion to catalyst walls (in the case of high catalyst activity), ammonia conversion is in the range of 95–100%. As one can see below, the active catalysts do achieve such conversion. It means that they operate in diffusion limited regime with a constant temperature along the catalyst length. In this case, measured selectivity towards NO and NO yield characterize intrinsic catalyst properties. If the tested catalyst does not show high ammonia conversion, it operates in a kinetic or in a partly diffusion regime. In this case NO yield is not only a catalyst kinetic characteristic. In spite of a short length of a sampling system exposed to high temperatures, a homogeneous reaction between ammonia and NO may take place in this space. This results in overestimation of ammonia conversion and underestimation of NO yield, measured NO yield being a relative value. Anyway the catalysts with a low conversion and a low NO yield are of less practical interest.

The ammonia conversion degree is in the range of 95–100% at 850–900 °C for all samples presented on Fig. 5a. However, NO yield strongly depends both on the chemical composition of the active component and preparation conditions (number of impregnations, nature of secondary sublayer, calcination temperature and so on) and on the catalyst temperature (Figs. 5–7).

The best NO yield for once impregnated perovskite catalysts was shown to be for Mn containing catalysts, but not exceeding 35% (Fig. 5b). Moreover, NO yield decreases with testing temperature. It is interesting that Co- and Cu-containing perovskite catalysts have higher NO yield in the temperature range 700–800 °C while Mn-containing catalysts show the best yield at temperature higher than 800 °C. Also, supported perovskite catalysts were shown to be more effective than supported simple oxides with corresponding Me cations. This fact indicates strong chemical modification of active components by support. Indeed, it is known that pure (not supported) MeO_x (Me = Fe, Co) and perovskites are characterized by rather high (80–96%) NO yields. And modification of pure oxides, for instance, by aluminum, magnesium and/or silicon oxides has always resulted in selectivity reduction, which may be due to changing optimal for NO formation Me–O bonding energy in oxides and perovskites [11].

A known method allowing to reduce the interaction between an active component and support is cordierite pre-covering by the secondary support. As a secondary support ZrO_2 , La_2O_3 , CeO_2 , Al_2O_3 are most frequently used [17,19,20]. We applied ZrO_2 , Ln_2O_3 (mixture of lanthanides – mish metal – $\text{Ln} = \text{La} + \text{Ce} + \text{Pr} + \text{Nd} + \text{Sm}$). In addition, we used once impregnated catalysts (pure oxide or perovskite) as secondary supports carrying out double impregnation.

In fact, the increase in the number of impregnations or impregnation of active component on the secondary sublayer independent of its chemical composition (Ln_2O_3 ,

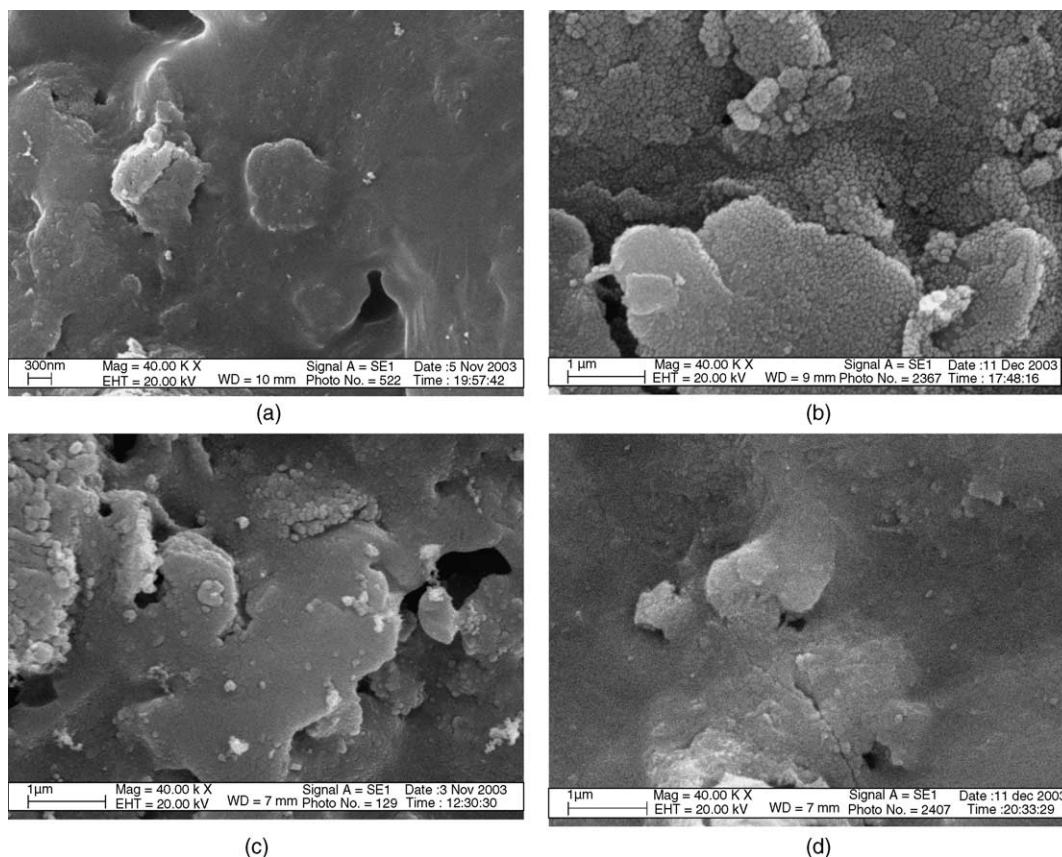


Fig. 3. SEM data on a carrier and on supported catalysts: (a) carrier, (b) carrier + Ln_2O_3 , (c) carrier + LaMnO_3 , (d) carrier + Ln_2O_3 + LaMnO_3 .

ZrO_2 , pure MeO_x , first layer of perovskite) leads to increase in NO yield as compared with catalysts without secondary sublayer (Fig. 6). It is interesting that NO yield on Co- and Cu-containing catalysts decreases with increase of catalyst testing temperature, while NO yield of Mn-containing catalysts goes through maximum at 800 °C and does not show such strong dependence on catalyst temperature. Hence, the most active catalysts in reaction of ammonia oxidation were found to be LaMnO_3 based supported on the

secondary layer or impregnated with an active component twice. Moreover, double impregnation makes NO yield less sensitive to the catalyst temperature.

Most probably, double impregnation or impregnation on the secondary sublayer (independently on its chemical composition) decrease a degree of the chemical modification of the active perovskite phase by aluminum, Mg, Si extracted from the cordierite substrate that increases the NO yield. Hence, cobaltites, manganites and cuprites of lanthanum are the most efficient at their content 5–6% or when supported on the secondary sublayer (Fig. 5.).

However, NO yields achieved are still lower than for pure perovskites [8,11] signifying chemical modification of active components by support material (cordierite). Thus, further investigations and development of supported catalysts for ammonia oxidation are prospective.

An important characteristic of a supported catalyst is its stability in operation conditions. Stability of the LaMnO_3 -based catalyst was tested by its life test inside a burner of the Russian high pressure nitric acid plant UKL-7 during 3 months. Four honeycomb monoliths with supported LaMnO_3 on cordierite with Ln_2O_3 sublayer were placed below a catalytic system. After 3 months running, neither change in the geometry nor cracks in the walls were observed. However, the color became lighter that may indicate the active layer modification. The specific surface

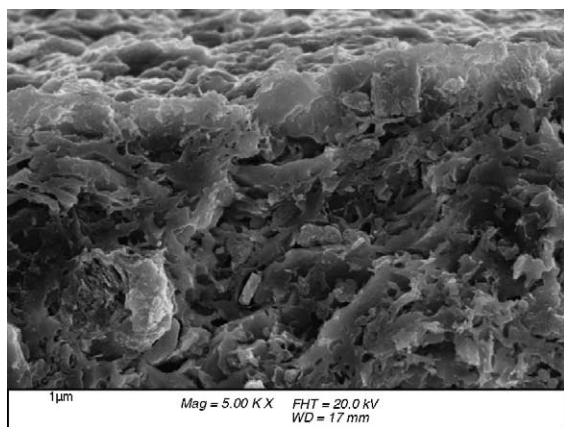


Fig. 4. SEM image of wall cross-section of cordierite with secondary Ln_2O_3 sublayer.

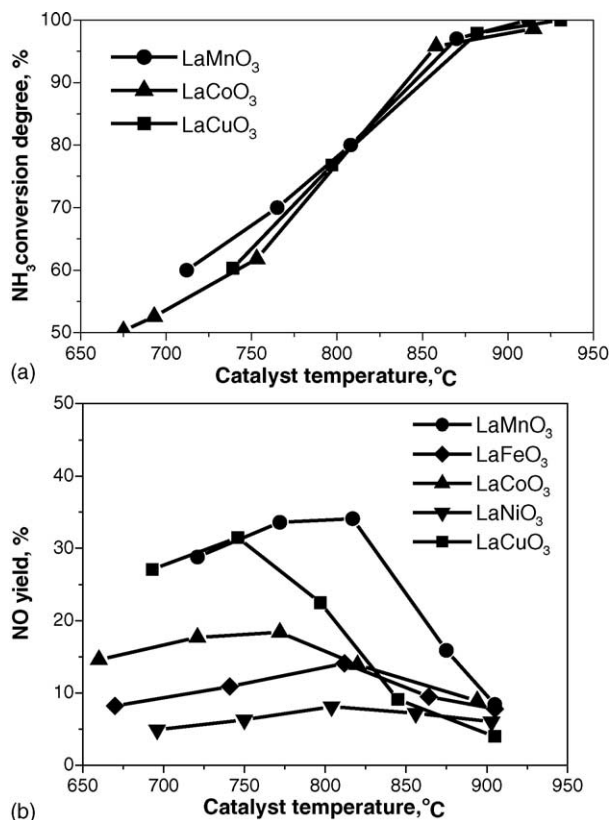


Fig. 5. Catalytic activity of LaMeO₃ supported (one impregnation stage) catalyst versus catalyst reaction temperature: (a) NH₃ conversion degree, (b) NO yield.

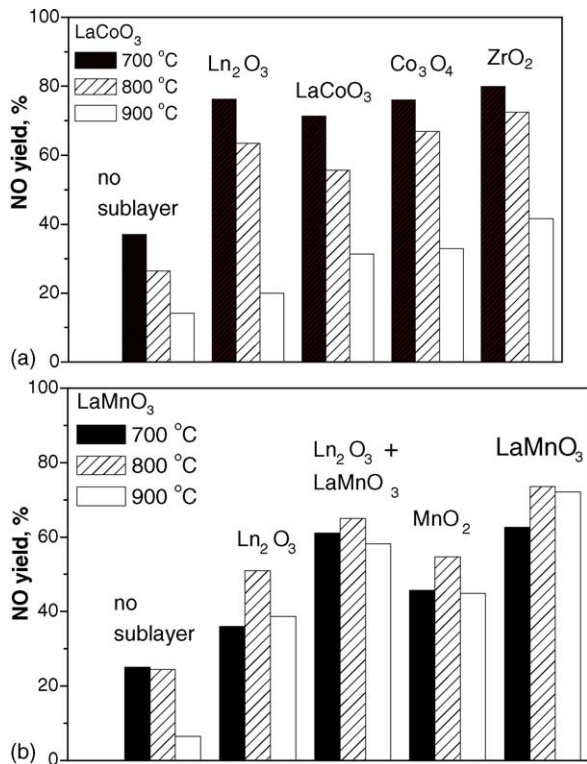


Fig. 6. NO yield at temperatures 700–900 °C for LaCoO₃ (a) and LaMnO₃ (b) based catalysts prepared with different secondary sublayers (sublayers compositions are in the pictures).

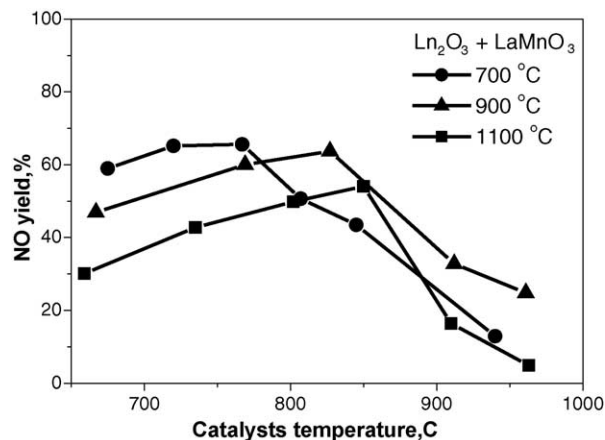


Fig. 7. NO yield for LaMnO₃-based catalyst prepared with Ln₂O₃ sublayer and calcined in the range 700–1100 °C vs. catalyst reaction temperature.

area has increased (from 1 to 1.6 m²/g), while the pore volume has decreased by 2 times (from 0.2 to 0.1 cm³/g). The testing of discharged samples revealed loss in activity and decline in NO yield as compared with the fresh sample (Fig. 8). The decline in selectivity observed may also be due to larger impact of homogeneous reactions in the sampling system.

According to X-ray phase analysis, a degree of cordierite (carrier) crystallinity decreased after the life test (intensity of the peak at $2\theta = 10^\circ$ decreases), but no strong change in intensity of the perovskite peak ($2\theta = 33^\circ$) was detected.

The chemical analysis of fresh and discharged catalysts has detected about 20% decrease of perovskite and sublayer formed cations content (from 1.36 to 1.09% (La), from 1.03 to 0.8% (Ce), from 0.47 to 0.36% (Mn)) in the sample after the life test. It may be noted also that in discharged samples precious metals (Pt, Pd and Rh) were detected; Pt and Pd content was lower than 0.001%, but Rh was in the amount of 0.03%. These metals are considered usually to vaporize from

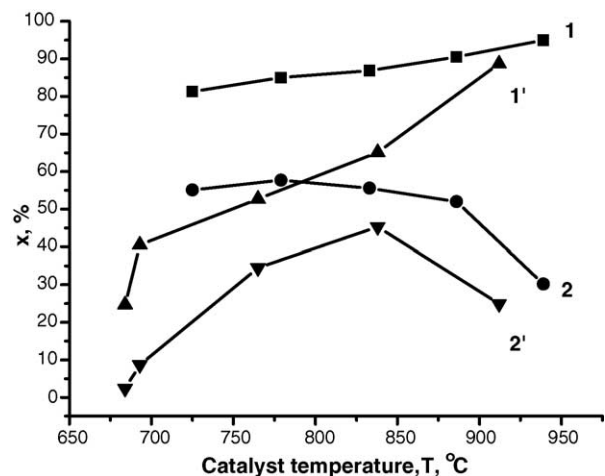


Fig. 8. NH₃ conversion (%) degree (1 and 1') and NO (%) yield (2 and 2') for fresh (1 and 2) and running for 3 months (1' and 2') LaMnO₃-based catalyst versus catalyst's temperature.

the gauzes and then to condensate on different walls. It is not excluded that Rh can be incorporated into the perovskite structure and effect catalyst properties as well. Hence, the change in the catalyst surface color may be both due to partial destruction of the active surface layer and the chemical interaction with the carrier.

4. Conclusions

Monolith honeycomb catalysts were prepared by supporting of honeycomb cordierite carrier with pure oxides and perovskites using Pechini method. A strong chemical interaction between active components and support was revealed by physical methods and catalyst testing in ammonia oxidation into NO. Efficiency of applying a secondary support was confirmed with a low effect of its chemical nature. The most promising are catalysts prepared by double perovskite impregnation or prepared by impregnation of perovskite on the previously supported oxide sublayer, which is explained by a less pronounced incorporation of aluminium cations into the lattice of perovskites. Stability of the prepared LaMnO_3 -based catalyst was checked by the 3-months life test in the high pressure ammonia plant. The catalyst has retained its mechanical properties but with loss of its initial activity. Further increase in NO yields is necessary to make the supported catalysts feasible for industrial application.

References

- [1] N. Yamazoe, J. Teraoka, *Catal. Today* 8 (1990) 175.
- [2] L.G. Tejuca, J.L.G. Fierro, J.M.D. Tascon, *Adv. Catal.* 36 (1989) 237.
- [3] E.J. Baran, *Catal. Today* 8 (1990) 133.
- [4] I. Rozetti, L. Forni, *Appl. Catal. B: Environ.* 33 (2001) 345.
- [5] J.G. McCarty, H. Wise, *Catal. Today* 8 (1990) 231.
- [6] D. Klvana, J. Vaillancourt, J. Kirchnerova, J. Chaouki, *Appl. Catal. A* 109 (1994) 181.
- [7] J. Petryak, E. Kolakowska, *Appl. Catal. B: Environ.* 24 (2000) 121.
- [8] Y. Wu, T. Yu, B.-s. Dou, C.-x. Wang, X.-f. Xie, Z.-l. Yu, S.-r. Fan, L.-c. Wang, *J. Catal.* 120 (1989) 88.
- [9] T. Yu, Y. Wu, G. Lü, W. Li, B. Lin, *Sci. Sin. B* 31/11 (1988) 1281.
- [10] A. Cybulski, J.A. Monlijin, *Catal. Rev.-Sci. Eng.* 36 (1994) 179.
- [11] V.A. Sadykov, L.A. Isupova, I.A. Zolotarskii, L.N. Bobrova, A.S. Noskov, V.N. Parmon, E.A. Brushtein, T.V. Telyatnikova, V.I. Chernyshev, V.V. Lunin, *Appl. Catal. A: Gen.* 204 (2000) 59.
- [12] V.A. Sadykov, E.A. Brushtein, L.A. Isupova, T.V. Telyatnikova, A.A. Kirchanov, I.A. Zolotarskii, A.C. Noskov, N.G. Kozevnikova, V.Y. Kruglyakov, O.I. Snegurenko, Y.N. Gibaddulin, A.A. Hazanov, *Khimicheskaya Promyshlennost'* (Chem. Ind.) 12 (1997) 33 (in Russian).
- [13] N.G. Kojevnikova, L.A. Isupova, V.Y. Kruglyakov, V.A. Sadykov, A.A. Kirchanov, A.A. Marchuk, M.A. Sadovnikova, A.S. Noskov, E.A. Brushtein, T.V. Telyatnikova, In book of abstracts of 2nd International Seminar «Monolith Honeycomb Supports and Catalysts», vol. 12–15, Novosibirsk, Russia, 1997, p. 118.
- [14] L.A. Isupova, V.A. Sadykov, E.A. Brushtein, T.V. Telyatnikova, N.G. Kojevnikova, V.Y. Kruglyakov, G.I. Storozhenko, In book of abstracts of 2nd International Seminar «Monolith Honeycomb Supports and Catalysts», vol. 12–15, Novosibirsk, Russia, 1997, p. 114.
- [15] V.I. Chernyshev, E.A. Brushtein, *Cataliz v Promyshlennosti* (Catal. Ind.) 3 (2001) 30 (in Russian).
- [16] S. Cimino, L. Lisi, R. Pirone, G. Russo, M. Turko, *Catal. Today* 59 (2000) 19.
- [17] S. Simino, S. Colonna, S. De Rossi, M. Faticanti, L. Lisi, I. Pettiti, P. Porta, *J. Catal.* 205 (2002) 309.
- [18] R. Schneider, D. Kießling, G. Wendt, *Appl. Catal. B: Environ.* 28 (2000) 187.
- [19] L. Fabrin, I. Rosetti, L. Forni, *Appl. Catal. B: Environ.* 44 (2003) 107.
- [20] N. Mizuno, H. Fujii, M. Misino, *Chem. Lett.* (1986) 1333.
- [21] D.L. Evans, G.R. Fisher, J.E. Geiger, F.W. Martin, *J. Am. Ceram. Soc.* 63 (1980) 629.
- [22] M.P. Pechini, U.S. Patent no. 3,330,697.
- [23] L.A. Isupova, G.M. Alikina, S.V. Tsybulya, A.N. Salanov, N.N. Boldyreva, E.S. Rusina, I.A. Ovsyannikova, V.A. Rogov, R.V. Bunina, V.A. Sadykov, *Catal. Today* 75 (1–4) (2002) 305.
- [24] E.F. Sutormina, *Zurnal Analiticheskoi Khimii* (J. Anal. Chem.) 59 (4) (2004) 1 (in Russian).